

MODELLING OF SAND OVER A WIDE STRESS RANGE USING FLAC

M.D. Bolton and M.W. Gui
Cambridge University Engineering Department
Trumpington Street
Cambridge CB2 1PZ
UK.

SYNOPSIS: A method has been derived for treating the triaxial data for sand which is useful for analysing piles and penetrometers or other situations in which significant stress levels vary from very high to very low. The data is divided into three categories; namely, the high, medium and low stress zones. These are separately modelled as zones of plastic hardening, in this case using the FLAC program. The consistency of the modelling is demonstrated by simulating triaxial tests. Application of this H-M-L model in the analysis of a cone penetration problem has also been demonstrated. Comparison with centrifuge results has been found to be encouraging, at least qualitatively.

1. INTRODUCTION

The strength parameters of sand (such as angle of shearing resistance ϕ , or angle of dilatancy ψ) are dependent on the mean effective stress. Bolton (1986) attributed this to the crushing strength of soil grains. Also, since the stresses involved in the penetration of a cone or a pile can vary from the far field insitu stress of a few kPa to the near field stress of a few MPa; it is necessary to have a stress dependent model that can be used over a wide stress range. The model could then be implemented numerically either through a finite element or a finite difference analysis. Nevertheless, no constitutive model for sand has yet been able to represent its stress-strain behaviour over a wide range of stresses.

An effort has therefore been made to escape the "parameter" problem by using raw triaxial data to define the plastic hardening of sand directly, and to use this in the numerical analysis of the cone penetration (Gui, 1995). This paper reveals a method to model triaxial data of sand over a wide stress range using FLAC.

2. FLAC

The finite difference program used in the following analysis is called FLAC (Fast Lagrangian Analysis of Continua). FLAC is an explicit finite difference programme which is well suited for modelling ill-behaved non-linear systems. The *double-yield* or *cap*

model in FLAC allows the user to represent arbitrary non-linear softening and hardening behaviour of the material and is based on the Mohr-Coulomb elastoplastic model with a non-associated flow rule. Parameters are given in terms of the variation with plastic shear strain of the apparent cohesion c , angle of friction ϕ , and angle of dilation ψ , all defined with respect to envelopes of Mohr circles. To cater for volumetric compaction, a volumetric yield function is also incorporated. On a (q, p') diagram, Fig 1, the parameters become Ω , η and i as functions of deviatoric strain ϵ_q , and p'_{cap} as a function of ϵ_v . The dilatancy angle i defined with respect to q, p' axes as shown in Fig 1 may be related to the plane angle of dilatancy ψ by: $\tan(i) = \sin(\psi)$.

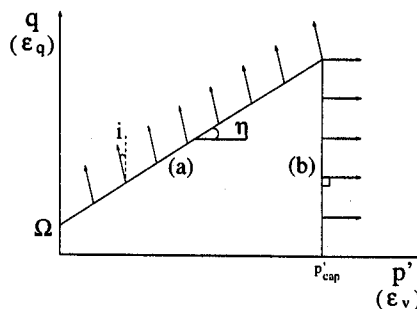


Fig 1: Double-yield model in FLAC: (a) shear yield surface; and (b) volumetric yield surface.

FLAC adopts the dynamic equations of motion so as to ensure that the numerical scheme would be stable

when the physical system which is being modelled is unstable. For details of the formulation of FLAC, readers are referred to the FLAC (1993) manual.

3. GENERALISATION OF TRIAXIAL DATA

Due to the difficulties in assigning thousands of different stress-strain curves to the individual elements of a numerical model, generalisation of the triaxial data is necessary. Triaxial data on 95% dense Fontainebleau sand produced by Luong and Touati (1983) are used here in the following fashion. Data points for shear strain at 0.5%, 1.0%, 2.0%, 4.0%, 8.0% and 16% are extracted and plotted in a (q, p') space as in Fig 2. It is intriguing to see that everyone of the (q, p') curves in Fig 2 does possess a unique shape as shown in Fig 3.

This unique shape shows that we can divide all the triaxial data into 3 pressure zones:

- Low pressure zone for $\sigma_3 < 0.5$ MPa
- Medium pressure zone for $0.5 \text{ MPa} < \sigma_3 < 6$ MPa
- High pressure zone for $\sigma_3 > 6$ MPa

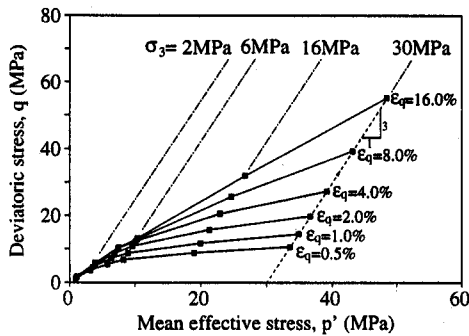


Fig 2: Triaxial data plotted in q-p' space.

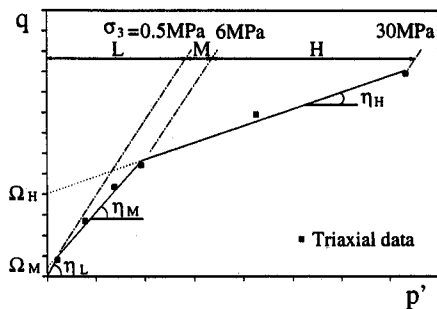


Fig 3: Definition of η and Ω in q-p' plot.

In this case, the high stress zone was defined by q, p' data from tests with $\sigma_3=30, 16$ and 6 MPa, to which the best straight line was fitted. The medium stress zone was treated similarly using data from the $6, 4, 2$ and 0.5 MPa tests, and the low stress zone was fitted using lines drawn between the origin and the data of the 0.5 MPa test.

Having divided the data into 3 zones, we can define:

$$q = \Omega + \eta p' \quad (1)$$

where η is the gradient of the q-p' line and Ω is the apparent deviatoric stress. The mobilised angle of friction ϕ , with respect to a particular strain level, can be calculated using the well known formula (Wood, 1990):

$$\phi = \sin^{-1} [3\eta/(6+\eta)] \quad (2)$$

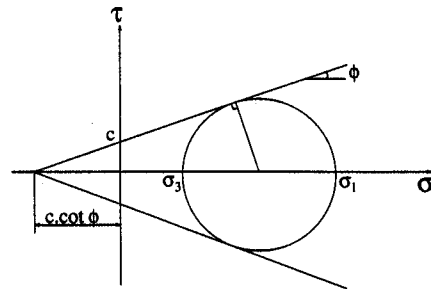


Fig 4: Mohr circle of stress.

From Fig 4, we can derive that:

$$(\sigma_1 + c \cdot \cot \phi) = (\sigma_3 + c \cdot \cot \phi) \tan^2(45^\circ + \phi/2) \quad (3)$$

Simplifying eqns (3), we get:

$$\sigma_1 = \sigma_3 \tan(45^\circ + \phi/2) + 2c \cdot \tan(45^\circ + \phi/2) \quad (4)$$

Substituting $q=(\sigma_1 - \sigma_3)$; and $p'=(\sigma_1 + 2\sigma_3)/3$ into eqn (4), we obtain the cohesion intercept:

$$c = \Omega / [2 \tan(45^\circ + \phi/2)(1-\eta/3)] \quad (5)$$

Armed with eqns (2) and (5), the relationship between both ϕ and c and plastic shear strain can be calculated, Fig 5 and 6. The dilation angle ψ is taken for simplicity to be:

$$\psi = \phi - 32^\circ \quad (6)$$

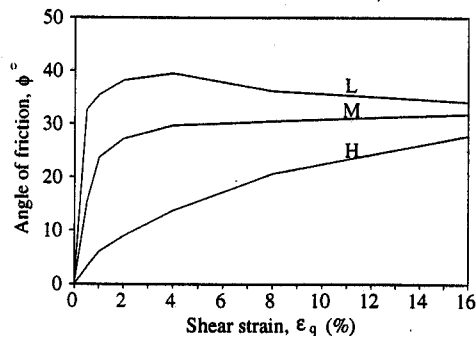


Fig 5: Mobilised ϕ with corresponding plastic strain.

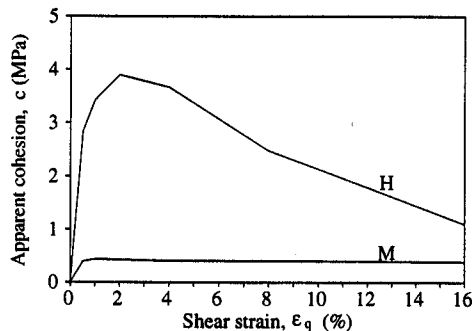


Fig 6: Apparent cohesion with corresponding plastic strain.

though it is recognised that regression lines could separately have been fitted to the various data of volumetric strains from the various triaxial tests in the same way as that used to define c and ϕ .

The second yield function for volumetric yield requires a relationship between the volumetric strain ϵ_v and the mean effective stress p' . The values shown in Fig 7 are taken from Luong and Touati (1983). It must be pointed out that due to the limitation of the *cap* model, no plastic volume loss would be predicted during a constant- p' test on normally consolidated soil. This conflicts with reality. It was decided to select the plastic volume change after both consolidation and shear stages of the tests, for entry to the model. The consequence is that we will over-estimate volume loss during isotropic consolidation, and then under-estimate volume loss during shear. However, soil reaching a critical state should be modelled reasonably well with respect to overall volume change.

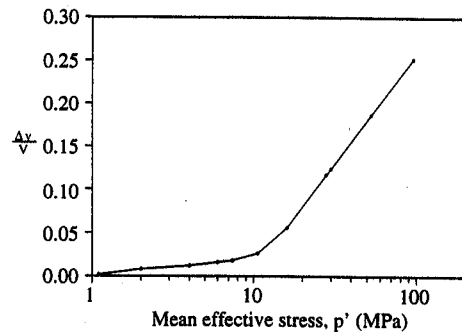


Fig 7: Volumetric strain with corresponding mean effective stress.

The elastic Young's moduli measured from the triaxial tests were 0.48×10^5 , 1.86×10^6 and 6.8×10^6 kPa for low, medium and high stress zones respectively. Poisson's ratio ν was taken to be 0.25.

4. MODELLING OF TRIAXIAL TEST

Seven simulation analyses have been performed using FLAC. The confining pressure ranges from 500 kPa to 30 MPa. Only half of the sample is modelled and it is divided into 50 elements (5×10). The top and bottom platens are fixed in both X and Y directions. A strain controlled test at a rate of 5×10^{-5} m/step is then applied to the sample.

FLAC results together with Luong and Touati's (1983) experimental results are presented in Fig 8 to 13.

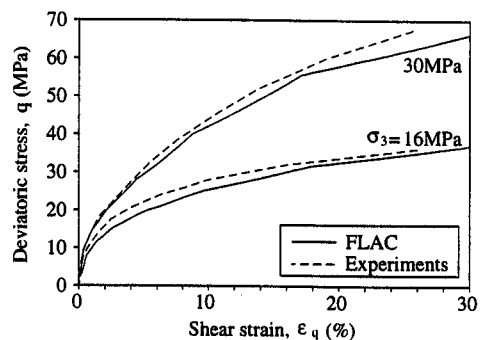


Fig 8: Result for high stress tests.

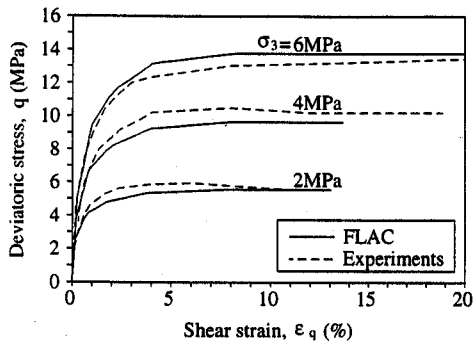


Fig 9: Result for medium stress tests.

It can be seen that the deviatoric stress q versus shear strain ϵ_q profiles match very well for all the tests in Fig 8, 9 and 10. Maximum deviation in deviatoric stress observed is no more than 10%. For the prediction of ϵ_v , as expected, the results only match in a global sense.

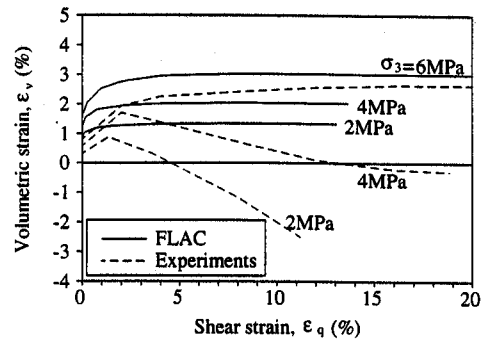


Fig 12: Volumetric strain for medium stress test.

For $\sigma_3 = 2$ and 4 MPa, Fig 12, FLAC predicted well the maximum volumetric strain in contraction. Thereafter, the values remain constant (no dilation). This is due to the input parameters we specified earlier. For these two tests ($\sigma_3 = 2$ and 4 MPa), the ϕ profile for medium stress test, Fig 5, indicated that there should be no dilation. Clearly, not all the subtleties of the influence of grain crushing on soil dilation have been captured.

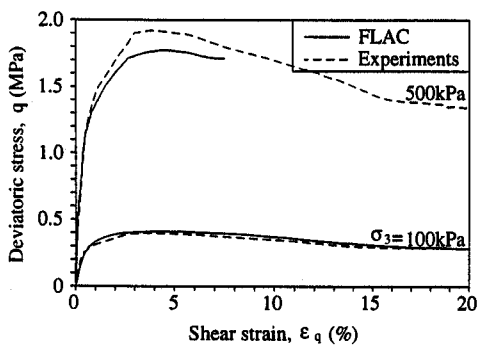


Fig 10: Result for low stress tests.

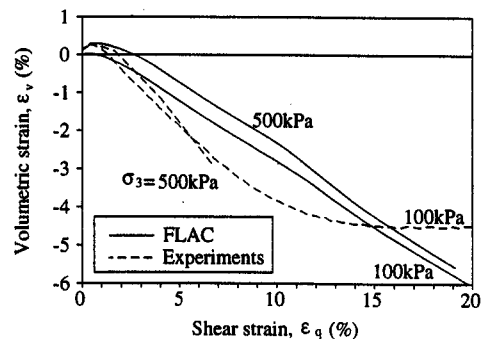


Fig 13: Volumetric strain for low stress test.

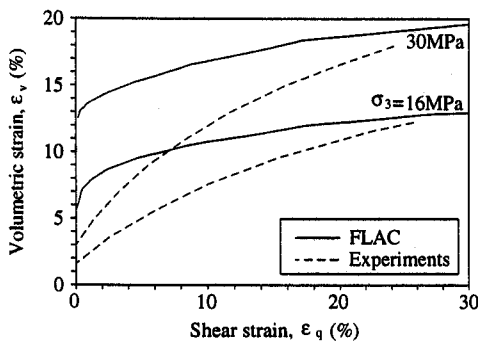


Fig 11: Volumetric strain for high stress test.

FLAC manages to predict both the contraction and dilation of the sample in the low stress test, Fig 13. Considering that the input parameters are derived for $\sigma_3 = 500$ kPa, the predictions are deemed to be acceptable.

5. MODELLING OF CPT

Having derived the H-M-L model, we can then apply it in the numerical simulation of a cone penetration test. The idealised numerical model is divided into 3 zones as in Fig 14.

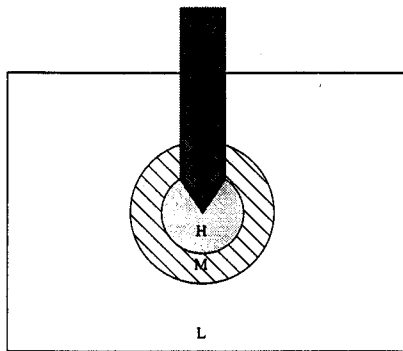


Fig 14: Idealised H-M-L zones in a CPT analysis.

The penetrometer is assumed to be installed deep in the ground by placing it in a pre-bored hole. The initial insitu stress is assumed to be undisturbed by the previous penetration. Using FLAC, a plastic indentation analysis is then carried out and the resulting pressure is identified with the cone resistance. An incremental displacement of 5×10^{-5} m/step is adopted in the analysis. The mean effective stress for each element is taken to be the average of σ_1 , σ_2 and σ_3 . Trial and error is necessary in order to define the boundaries for all the pressure zones. A details description of the simulation procedures can be found in Gui (1995).

FLAC results together with a cone profile from a centrifuge test on dense Fontainebleau sand are plotted in Fig 15. Qualitatively, the H-M-L model produces a similar profile to those obtained in the centrifuge, at least for the first 10m of penetration.

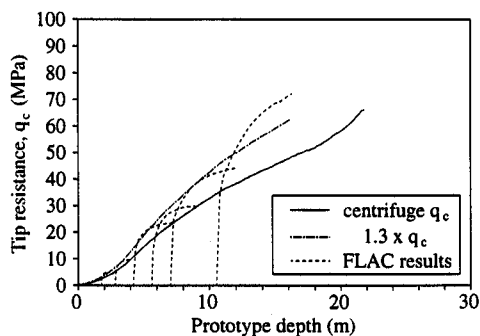


Fig 15: Predicted and experimental cone profile

The overestimation of the cone resistance may be due to the fact that an element beneath the cone is not subjected to a true triaxial condition, making the triaxial data unrepresentative of the true strength of the soil. Furthermore, the use of a more realistic shape

of yield surface could influence the calculation since volumetric contraction could occur at lower stress ratios. Finally, the rate of post-peak softening of sand in the low stress zone will inevitably be related to the geometry of rupture bands which will relate to the size of soil particles, and will depend on the precise failure kinematics.

The advantage of this direct style of modelling is, however, that the sensitivity of the final resistance to the properties of the sand (stiffness in the far field at small strain and small stress levels, strength in the medium field with dilatancy at middling stress levels, and volumetric contraction due to crushing at high stress levels in the near field) is easily determined. Only then can proper calibration between CPT data and selected "soil parameters" be made.

6. CONCLUSION

In general, the H-M-L model gives a good prediction of deviatoric stress and strain. Due to the limitation of the *cap* model, the prediction of the volumetric strain is only deemed satisfactory. The application of this H-M-L model in the numerical simulation of the cone penetration or pile problem has been proven to be successful.

7. REFERENCES

1. Bolton, M.D. (1986) The strength and dilatancy of sands. *Geotechnique* 36(1), p65-78.
2. FLAC (1993) ver 3.22 User Manual.
3. Gui, M.W. (1995) Centrifuge and numerical modelling of cone penetration tests/piles in sand. PhD Thesis, Cambridge University, UK. (to be submitted)
4. Luong, M.P. and Tuoati, A. (1983) Sols grenus sous fortes contraintes. *Revue Francaix de Geotechnique*, 23, p51-63.
5. Wood, D.M. (1990) Soil behaviour and critical state soil mechanics. Cambridge University Press, UK.